

Chapter 4

Results and discussion

Coal tar pitch characterisation and mathematical prediction of characteristics

4.1 CTP characterisation

4.1.1 Fundamental properties of CTP

Knowledge of the fundamental properties of CTPs is essential in the carbon processing and ferroalloy industries. These properties are widely used to determine the performance of CTP in various carbon processing industries [Alcañiz-Monge et al., 2001] and they have an influence on the thermal behaviour of CTP [Guillen et al., 1995; 1996]. Manoj and Kunjomana. [2012] reported that the structure and properties of coal and coal-related products have a direct effect on conversion processes such as liquefaction, pyrolysis and gasification.

The main fundamental properties of CTP that have been widely reported in literature include parameters such as softening point (SP), coking value (CV), quinoline insolubles (QI) and toluene insolubles (TI) [Bhatia et al., 1987; Alcañiz-Monge et al., 2001]. These parameters can be analysed by making use of various methods, as described in section 3.2

In Table 4.1, the fundamental properties of the 12 CTP samples evaluated during this study are presented. The SP of CTP provides an indication of the lowest temperature at which a CTP softens when heated at a constant rate. CTP 1 and 8 had the highest SP of 121.2 °C and 134.2 °C, respectively, with the remainder of the samples having SPs ranging from 65.4 to 94.6 °C. According to literature [Codd et al., 1971; Conroy et al., 1975; Stadelhofer et al., 1982], the recommended SP range of CTPs, used as binder and impregnation pitches, lies between 80 and 150 °C . Bhatia et al. [1987] reported that pitches characterised by high SPs

are suitable for use in the manufacture of carbon composites, and Yu et al. [2012] reported the suitability of high SP as spinnable pitches.

Table 4.1 Fundamental properties of CTP samples

Sample identity	SP (°C)	CV (%)	QI (%)	TI (%)
CTP 1	121.2	56.9	6.6	26.3
CTP 2	81.9	37.1	3.6	16.0
CTP 3	66.5	37.2	3.7	16.2
CTP 4	94.1	46.8	4.5	20.0
CTP 5	94.6	47.5	4.6	19.1
CTP 6	65.6	41.5	3.8	20.0
CTP 7	82.6	47.6	5.4	24.0
CTP 8	134.2	60.3	7.0	34.6
CTP 9	83.1	43.0	2.9	23.7
CTP 10	93.8	50.0	5.8	18.2
CTP 11	65.4	46.6	7.3	22.2
CTP 12	85.0	48.7	7.2	23.2

SP: softening point

QI: quinoline insolubles

CV: coking value

TI: toluene insolubles

The CV represents the amount of carbonaceous material that remains when all the volatile components in a CTP sample have been evolved (see Section 3.2.2 for the CV determination experimental procedure). It is reported in literature that the CV of CTP lies between 34 and 65% [Conroy et al., 1975]. From the analysed samples, the CV ranged from approximately 37% to a maximum of approximately 60%. Pitches with high CVs are used mainly in the manufacture of carbon composites [Bhatia et al., 1987].

The QI and TI contents quantify the organic/inorganic material that does not dissolve in these solvents. The insoluble particles are either formed in the coke oven, or carried over during distillation of the CTP in the coke oven. The QI content also provides additional information on the sizes of molecules in the CTP, with higher QI being an indication of larger molecules in a sample [Currie et al., 1955]. CTPs 11 and 12 had the highest QI contents, with CTP 8 having the highest TI.

The fundamental properties of the CTPs evaluated during this study varied considerably (Table 4.1) and the range of values obtained is larger than what has been reported in literature [Guillen et al., 1996; Diaz and Blanco, 2003; Yu et al., 2012]. These diverse sample compositions were obtained intentionally, to enable the evaluation of the hypotheses developed in this study for CTPs with a wide range of compositions.

4.1.2 Proximate analysis of CTP

In Table 4.2, the proximate analysis values for the 12 CTP samples are presented. CTP 8 had the highest FC and lowest volatile contents, while CTP 2 had the lowest FC and highest volatile contents. The volatile matter and ash content reported are slightly higher than what have been reported in literature [Machnikowski et al., 2006; Galiguzov et al., 2012]. The fixed carbon content is in agreement with what is reported in literature [Machnikowski et al., 1997, 2006].

Table 4.2 Proximate analysis of CTPs on an air dried basis

	Moisture (%)	Volatiles (%)	Ash (%)	FC (%)
CTP 1	0.2	55.6	0.4	43.8
CTP 2	0.6	69.8	0.5	29.1
CTP 3	0.7	65.2	0.7	33.4
CTP 4	0.2	63.6	0.4	35.8
CTP 5	0.3	63.4	0.5	35.8
CTP 6	1.0	62.8	0.9	35.3
CTP 7	0.6	69.0	0.8	29.6
CTP 8	0.2	51.4	0.2	48.2
CTP 9	0.2	64.3	0.3	34.9
CTP 10	0.2	59.5	0.6	39.7
CTP 11	0.1	60.7	0.5	38.7
CTP 12	0.1	58.1	0.5	41.3

FC: Fixed carbon content

4.1.3 Ultimate analysis of CTP

The ultimate analysis results that are summarised in Table 4.3 indicate a wide variation in the elemental composition of all samples, with carbon and hydrogen being the dominant elements in all the samples. The sulphur content is very low in all 12 samples, averaging approximately 0.5%. CTP samples characterised by low sulphur content are deemed environmentally friendly as they will result in low emissions of sulphur-related compounds during thermal treatment [Alcañiz-Monge et al., 2001]. The nitrogen contents were also low, with an average of 1.15% for all samples. The oxygen content varied considerably among the different samples. These differences can mainly be attributed to the different fractional occurrences of hydroxyl, phenolic, methoxy and carbonyl groups present in the samples

[Alcañiz-Monge et al., 2001; Speight, 2005]. The ultimate analysis results for all 12 samples analysed are comparable to what other researchers have found [Fitzer et al., 1987; Bermejo et al., 1995; 1997; Alcañiz-Monge et al., 2001; Mendez et al., 2008; Galiguzov et al., 2012]

Table 4.3 Ultimate analysis of CTP samples on a dry ash free basis

Sample	C (%)	H (%)	N (%)	S (%)	O (%)	C/H
CTP 1	90.80	4.16	1.15	0.49	3.40	1.81
CTP 2	91.54	4.13	1.17	0.49	2.67	1.84
CTP 3	91.98	4.03	1.13	0.53	2.33	1.90
CTP 4	90.72	4.23	1.19	0.53	3.33	1.73
CTP 5	91.27	4.36	1.17	0.53	2.67	1.84
CTP 6	90.32	4.33	1.25	0.55	3.55	1.74
CTP 7	91.43	4.12	1.15	0.50	2.80	1.84
CTP 8	93.38	3.23	1.15	0.50	1.74	2.42
CTP 9	91.38	4.35	1.14	0.50	2.63	1.75
CTP 10	91.23	3.89	1.16	0.49	3.23	1.95
CTP 11	91.01	4.19	1.18	0.50	3.12	1.81
CTP 12	91.06	3.85	1.17	0.53	3.39	1.97

4.2. Additional chemical composition determination of CTP

CTP is a complex mixture of hydrocarbons with different molecular weights and chemical functional groups [Lewis, 1982, 1987; Guillen et al., 1995, 1996; Machnikowski et al., 1997; Burgess and Thies, 2011; Yu-ying et al., 2010]. The complex nature of CTP makes it difficult to get the accurate chemical composition of the material [Diaz and Blanco, 2003]. Effective pitch characterisation makes it easier to understand the environmental impact of different conversion processes, allows for the identification and separation of different types of pitches, broadens the scope of pitch application, and makes it much easier to understand their thermal behaviour for industrial applications [Martin et al., 1998; Blanco, 2000]. It is also

reported that the pitch composition has an influence on the chemical and physical properties of the different end products [Bermejo et al., 1995]. In order to get useful information on the chemical composition of CTP, a number of additional analytical techniques, such as HPLC, GC-MS, NMR and FT-IR, can be used [de Castro, 2006].

NMR spectroscopy is used to determine the pitch aromatic and aliphatic fractions [Martin et al., 1998; Alcañiz-Monge et al., 2001] (section 3.4.1). FT-IR is useful in mainly the qualitative identification of the various functional groups within CTP samples, as well as following structural changes that take place during thermal treatment [Guillen et al., 1992; Machnikowski et al, 1997] (Section 3.4.2).

4.2.1 NMR analysis of CTP

NMR can be used to categorise CTPs according to the major structural parameters that can be analysed. During this study, 12 CTP samples were analysed by NMR, as described in section 3.5.1. The different structural parameters were calculated, as described by Solum et al. [1989] and are illustrated in Table 4.4. From the results, it is evident that all the samples are characterised by a reasonably high aromatic fraction averaging 0.96, while the aliphatic fraction for all samples averages only 0.04. Furthermore, all samples are characterised by a high fraction of non-protonated carbons in the aromatic region (f_a^N) averaging 0.6 for all samples. The fraction of phenolics (f_a^P) is low for all samples and the same applies for the fraction of alkylated aromatics (f_a^S). The variations that occur between the aromatic and aliphatic contents of all CTP samples are illustrated in the NMR spectra shown in Figure. 4.1.

Table 4.4 Calculated structural NMR parameters for the 12 CTP samples

	CTP 1	CTP 2	CTP 3	CTP 4	CTP 5	CTP 6	CTP 7	CTP 8	CTP 9	CTP 10	CTP11	CTP 12
f_a	0.96	0.95	0.91	0.98	0.97	0.96	0.99	0.97	0.96	0.97	0.97	0.96
f_a^*	0.90	0.90	0.87	0.90	0.90	0.89	0.91	0.90	0.89	0.91	0.91	0.90
f_{al}	0.04	0.05	0.09	0.02	0.03	0.04	0.01	0.03	0.04	0.03	0.03	0.04
f_{al}^O	0.00	0.00	0.02	0.00	0.00	0.00	0.00	0.00	0.00	0.00	0.00	0.00
f_a^{CO}	0.00	0.00	0.00	0.00	0.00	0.00	0.00	0.00	0.00	0.00	0.00	0.00
f_a^P	0.02	0.02	0.01	0.02	0.02	0.03	0.01	0.01	0.03	0.03	0.03	0.03
f_a^S	0.12	0.13	0.10	0.12	0.12	0.13	0.11	0.09	0.14	0.15	0.14	0.15
f_a^N	0.68	0.61	0.52	0.67	0.58	0.59	0.63	0.65	0.64	0.70	0.64	0.70
f_a^H	0.21	0.29	0.35	0.23	0.32	0.31	0.28	0.25	0.27	0.20	0.27	0.20
f_a^B	0.55	0.46	0.41	0.52	0.43	0.42	0.50	0.56	0.48	0.52	0.48	0.52
$f_{al}^{N^*}$	0.00	0.00	0.00	0.00	0.00	0.00	0.00	0.00	0.00	0.00	0.00	0.00
f_{al}^H	0.04	0.05	0.09	0.02	0.03	0.04	0.01	0.03	0.03	0.03	0.03	0.04
X_b	0.61	0.51	0.47	0.58	0.49	0.48	0.55	0.62	0.55	0.52	0.52	0.57
C	39.8	25.4	23.2	32.8	23.8	23.2	28.9	41.2	29.2	28.5	25.9	31.7
#Clusters/100	2.25	3.55	3.74	2.74	3.77	3.84	3.14	2.19	3.05	3.18	3.53	2.83
$\sigma + 1$	5.89	4.24	2.87	5.30	3.75	4.22	3.98	4.32	4.77	5.13	4.75	6.33

f_a : fraction aromatics

f_a^S : fraction alkylated aromatics

X_b : Mole fraction

f_a^* : corrected fraction aromatics(excl CO)

f_a^N : fraction non-protonated C's in aromatic

Clusters/100: #clusters/100 carbons

f^{al} : fraction aliphatic

f_a^H : fraction of protonated C's in aromatic region $\sigma + 1$: no of attachments per cluster

f_a^O : fraction aliphatic C's bonded to oxygen

f_a^B : fraction of bridgehead C's

f_a^{CO} : Fraction CO

$f_{al}^{N^*}$: fraction non-protonated C's +methyl groups in aliphatic region

f_a^P : fraction phenolic

f_{al}^H : aliphatic CH + CH₂

All CTP samples were characterised by similar NMR spectra. The NMR spectra of CTP 2, 9 and CTP 12 were selected at random and are shown in Figure 4.1. Samples whose NMR spectra are not shown in Figure 4.1 are included in Appendix 2.

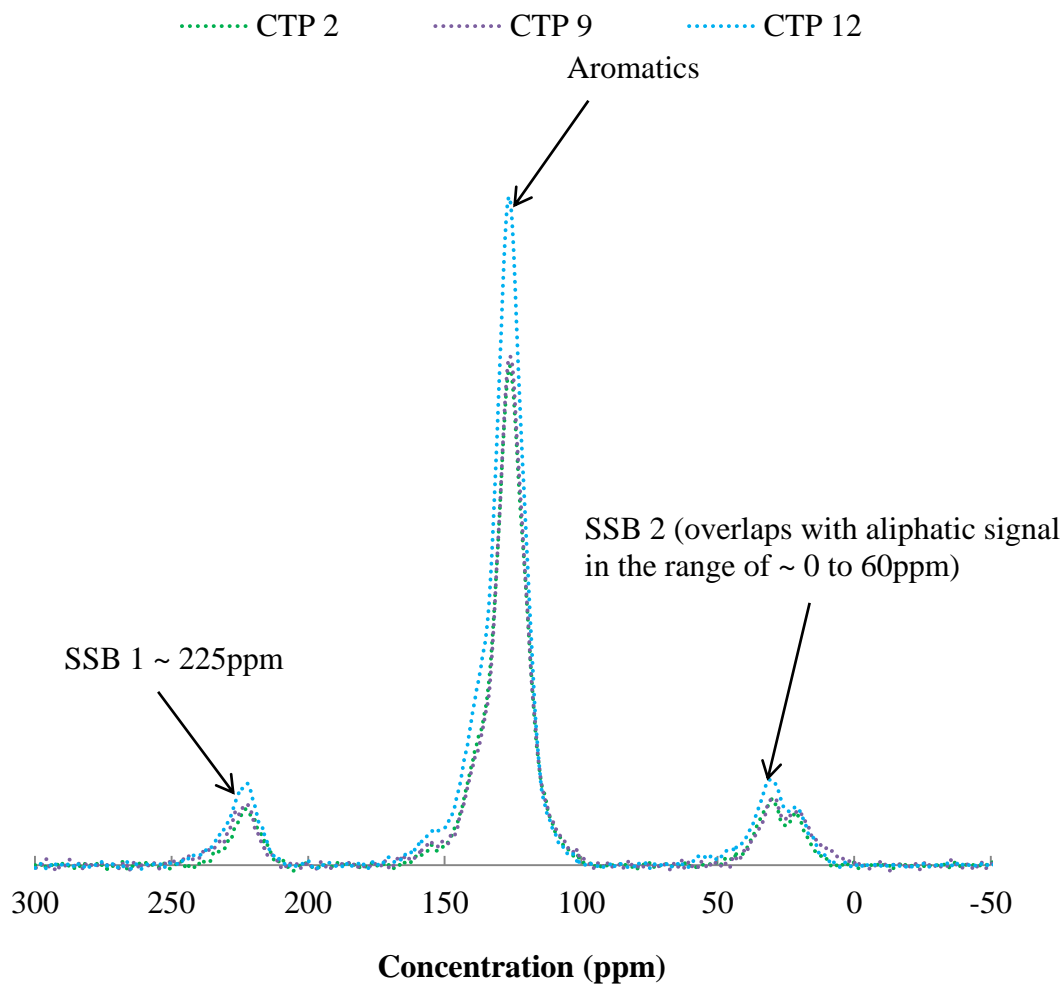


Figure 4.1 Typical CP MAS spectra of a CTP samples

From the results obtained, it was found that the NMR spectra for all 12 raw (as-received) CTP samples were similar, with the only differences being the peak intensities. The differences in peak intensity are due to the fractional variations in the functional group content among the

different samples. This observation was also confirmed by FT-IR analysis (section 4.2.2). According to Solum et al. [1989], chemical shifts ≥ 90 ppm are indicative of the aromatic region. Diaz and Blanco. [2003] reported that the NMR analysis of CTP is characterised by an aromatic region that lies in the chemical shift range of 150 to 108 ppm. From Figure 4.1, the large sharp peak is characteristic of the aromatic peak stretching from 110 to 150 ppm with a peak maximum at 120 ppm. Andresen et al. [1998] found that the aromatic peak occurred at a chemical shift of 125 ppm. The aliphatic peak is smaller and it overlaps with the spinning side band in the chemical shift range of 0 to 60 ppm. The different chemical shifts observed in CTP are illustrated in Table 4.5.

Table 4.5 NMR chemical shift descriptions [Diaz and Blanco, 2003; McMurry, 1992]

Symbol	Description	σ ppm
C_{ar}	Cata-condensed aromatic carbons	160-129.5
	Aromatic Cs joined to aliphatic chains	129.5-108
	Peri-condensed and protonated aromatic carbons	
C_{al}	Methylene carbons in α position to the aromatic ring	49.3-34
	All methylene carbons	34-23
	Methyl carbons	23-17

C_{ar} is aromatic carbons, while C_{al} is for aliphatic carbons

4.2.2 FT-IR analysis

The successful identification of different functional groups within a sample with FT-IR depends on the correct IR band allocation [Alcañiz-Monge et al., 2001]. Table 4.6 provides some IR

absorptions for different functional groups [McMurry, 1992; Guillen, 1995; Stuart, 1996; Papole et al., 2012].

Table 4.6 FT-IR functional group identification

Band position (cm ⁻¹)	Functional groups present
3640 - 3400	Alcohols (O-H)
35100-3310	Amines(N-H)
3100-3020	Alkenes(= C-H)
2960-2850	Alkanes and alkyl groups
3300	Alkynes
2260-2200	Nitriles
1780-1670	Carbonyl compounds
3100-2500	Carboxylic acids
3030	Aromatics
2400	Phosphorus
2200	Silica
2143	CO ₂
1000-700	Out of plane C-H bending vibrations
1600-1500	Aromatic rings
1400-1000	- C – O bonds

In this study, 12 CTPs were analysed with FT-IR, as described in section 3.4.2. The FT-IR spectra for all 12 raw pitch samples were similar, with only the band intensities differing. For illustration purposes, the FT-IR spectra of CTP 1 and CTP 3 were selected at random and are shown in Figure 4.2 below.

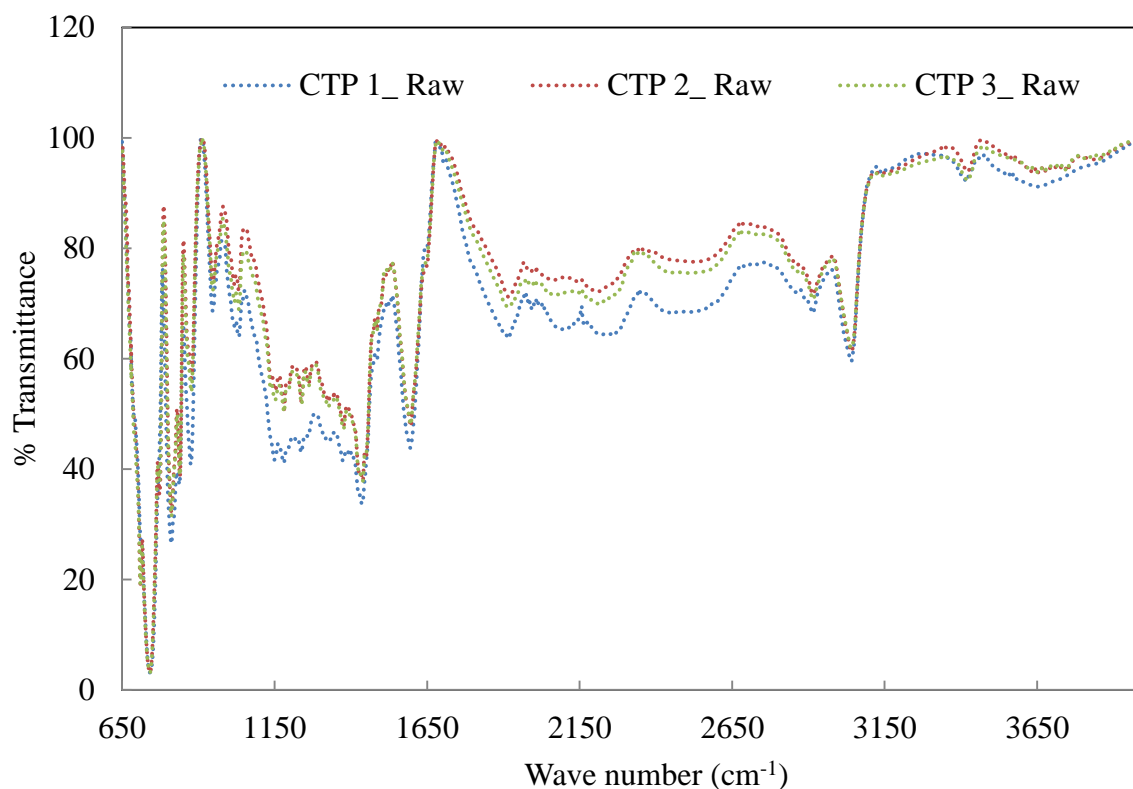


Figure 4.2 FT-IR spectra of raw (as-received) CTP 1, 2 3

As stated above, the FT-IR spectra of all 12 CTP samples analysed were found to be similar, with the only difference being the intensity of the peaks. The differences in peak intensities are due to varying quantities of the different functional groups in the samples. The FT-IR spectra obtained for all samples confirm the presence of N-H groups, which are indicated by the peak at 3412 cm^{-1} [Guillen et al., 1992, 1995]. The stretching from 3853 , 3752 , 3622 and 3412 cm^{-1} is due to the presence of O-H groups within the samples [Stuart, 1996; Prauchner et al., 2001; Geng et al., 2009]. 3040 cm^{-1} is characteristic of aromatic bands showing unsaturation [Martin et al., 1989; Geng et al., 2009]. FT-IR bands ranging from 2970 to 2850 cm^{-1} are due to aliphatic and alicyclic CH_3 , CH_2 and CH [Prauchner et al., 2001]. The peak at 1594 cm^{-1} is due to $\text{C}=\text{O}$

aromatic, C=C and C=C groups [Painter et al., 1985; Guillen et al., 1992]. 1436 cm^{-1} indicates CH_3 deformation and CH_2 bridges. Peaks observed in the range of 880 to 750 cm^{-1} are due to aromatic stretching. The FT-IR results reported in this study are similar to those reported by Painter et al., 1985; Guillen et al., 1992; 1995; Alcañiz-Monge et al., 2001. The authors observed N-H stretch at 3400 cm^{-1} , aromatic CH groups 3100 and 3000 cm^{-1} , and aliphatic hydrogen peaks between 2800 and 2980 cm^{-1} . C=O vibrations were also observed in the region 1800 to 1600 cm^{-1} . Aromatic out-of-plane vibrations were also noted in the region 880 to 750 cm^{-1} .

4.2.3 XRD analysis of raw CTP samples

XRD is widely used in the determination of the crystallinity of carbonaceous materials, as well as the degree of ordering (DOG) in a given material. The interlayer spacing between graphene layers can also be determined in coal and coal-related products, such as CTP [Hussain and Qadeer 2000; Tagaki et al., 2004; Van Niekerk et al., 2008; Manoj and Kunjomana, 2012] (section 3.6.1).

In this study, 12 CTP samples were analysed by XRD as described in section 3.6.1. All 12 CTP samples had a similar diffraction pattern. In Figure 4.6, the diffraction patterns of CTP 1, CTP 6 and CTP 10 are shown, as examples of the results obtained.

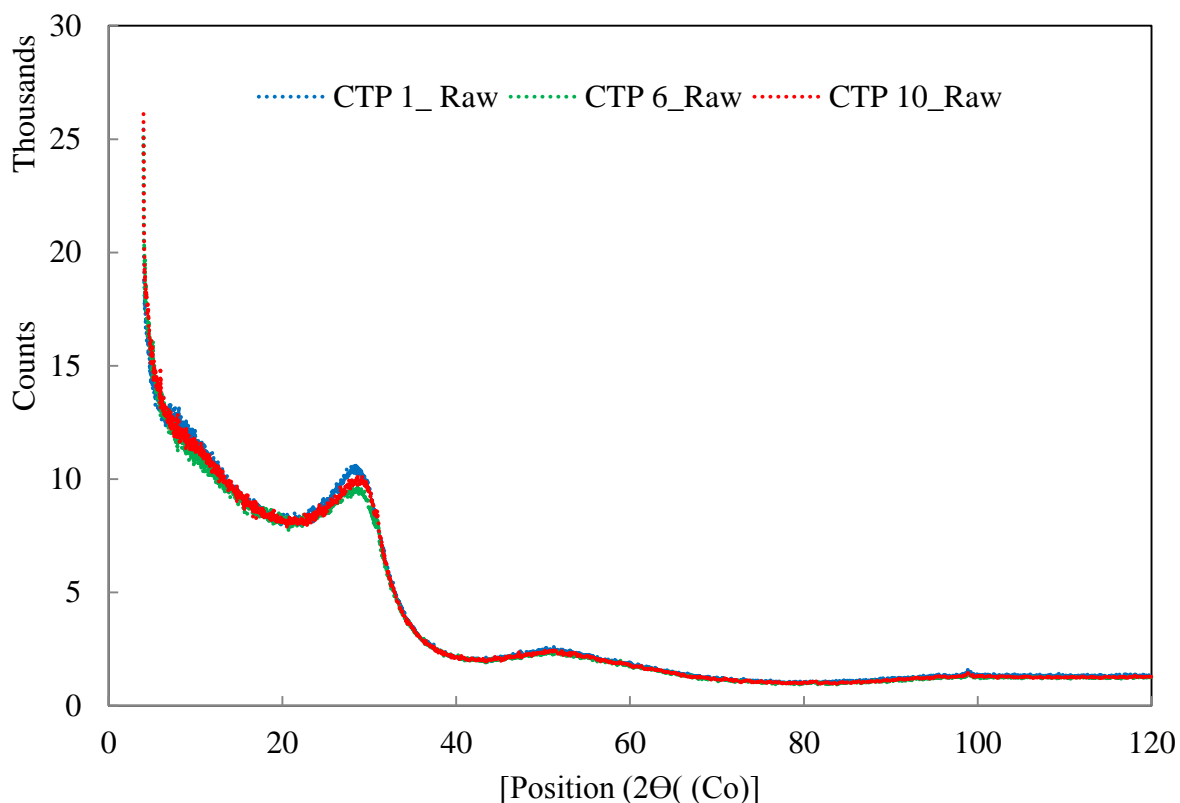


Figure 4.3 XRD diffractograms of raw (as-received) CTP

As can be seen in Figure 4.3, there is a relatively stronger and sharper XRD diffraction peak at 2θ values of 20 to 40 ° and also a very weak peak at 2θ value of 100 °. The XRD diffraction spectra can be used to quantify crystallinity [Feret et al., 1998; Tagaki et al, 2004]. From Figure 4.3 and d-spacing values for raw CTP reported in Table 6.2, it can be concluded that there is no crystallinity observed in any of the 12 raw pitch samples analysed. Using the equation described in section 2.6.6 used to calculate DOG, the average calculated DOG for all raw CTP samples was negative which is an indication that the raw CTP is an amorphous material with no structural ordering in it (no graphitization).

4.3 Predicting/calculating less commonly conducted CTP characteristics

Certain characteristics of CTPs are quite easily measured, such as the SP (Section 3.2.1), as well as the proximate and ultimate analyses (Section 3.3). However, other important parameters such as the CV, TI and QI contents are time consuming (Section 3.2.2 to 3.2.4) and involve the use of harmful solvents, such as toluene and quinoline in some of these analyses. It would therefore be very useful if these less commonly measured parameters, i.e. CV, as well as TI and QI contents, could be predicted or calculated.

4.3.1 Multi-linear regression to calculate/predict CV

The basic principles of multi-linear regression (MLR) calculations were discussed in section 3.7. The relationships between the optimum numbers of variable combinations obtained as the optimum solution during the multi-linear regression analysis for calculating/predicting the CVs of the CTPs are indicated in Figure. 4.4. The y-axis of this figure indicates the root mean square error (RMSE) difference between the experimentally determined CVs and the multi-linear regression determined CVs. As is evident from these results (Figure 4.4), a linear equation containing only the single most optimum variable had an RMSE of ~3.4. The RMSE could, however, be lowered to ~2.6 if a multi-linear equation containing the best combination of two variables was calculated. Similarly, this optimum combination of variables in the multi-linear equation gave progressively smaller RMSE values as the number of variables increased in the optimum solution. However, the inclusion of more than seven parameters into the multi-linear regression did not yield significantly lower RMSE values. The optimum combination of variables included in the multi-linear regression for CV calculation/prediction was therefore 7, with these variables being SP, FC, Ash, Volatiles, H, N and S.

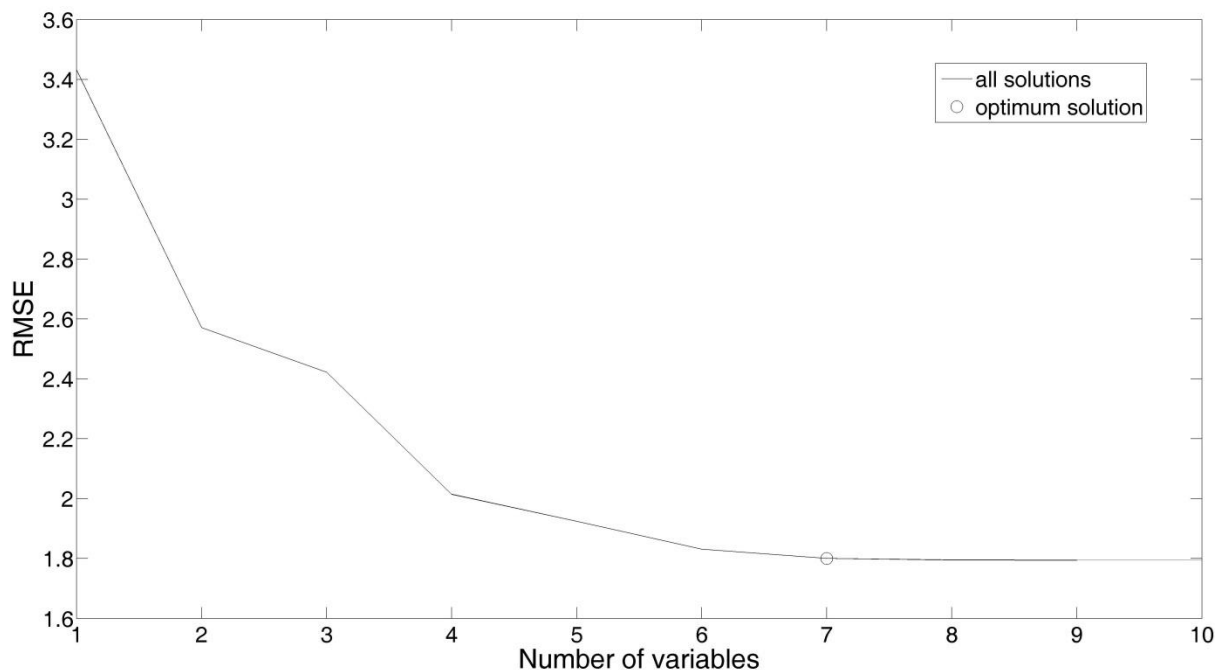


Figure 4.4 RMSE as a function of optimum combination of parameters used in the multi-linear regression calculation/prediction of CV

From the above-mentioned determination of the optimum number of variables to include in the multi-linear regression (Figure. 4.4), the actual multi-linear regression equation can be obtained.

This multi-linear regression equation to calculate CV for CTPs is:

$$CV = -1132.48 + (0.26 \times SP) + (11.46 \times \text{Proximate FC content}) + (31.62 \times \text{Proximate ash content}) + (11.08 \times \text{Proximate volatile content}) + (-3.18 \times \text{Ultimate H content}) + (44.12 \times \text{Ultimate N content}) + (-22.85 \times \text{Ultimate S content})$$

Utilising the above-mentioned equation, the CVs for the various CTPs were calculated and compared to the experimentally determined CV values. This comparison is shown in Figure 4.5.

As is evident from Figure 4.5, multi-linear regression can be used very successfully to calculate/predict the CV values of a CTP, utilising the SP, as well as proximate and ultimate analysis values.

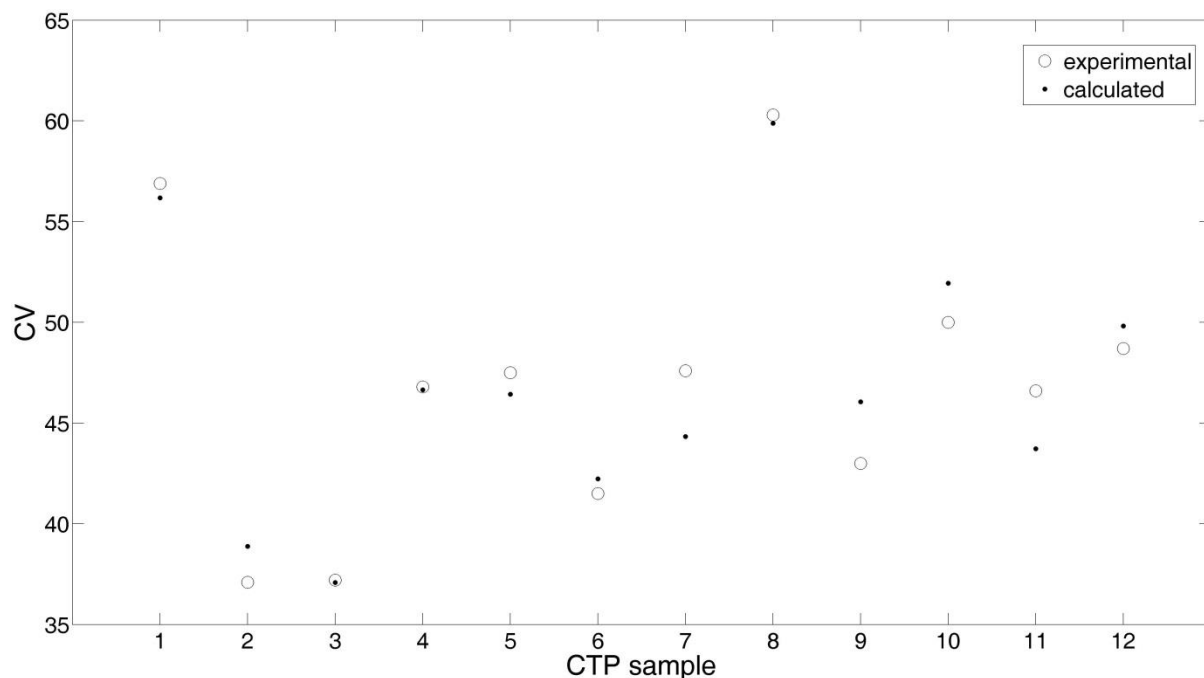


Figure 4.5 Comparison of CV values determined experimentally and those calculated utilising multi-linear regression

4.3.2 Multi-linear regression to calculate/predict TI

The determination of the optimum number of variables to include in the MLR equation analysis results for TI is shown in Figure 4.6. From the figure, it is evident that the RMSE calculated with a single optimum variable was ~3.4. This was reduced to ~3 when the best combination of the two most optimum variables was used. However, the RMSE could be minimised by including the best combination of nine variables to predict TI. These variables were SP, Moisture, Ash, Volatiles, C, H, N, S and O.

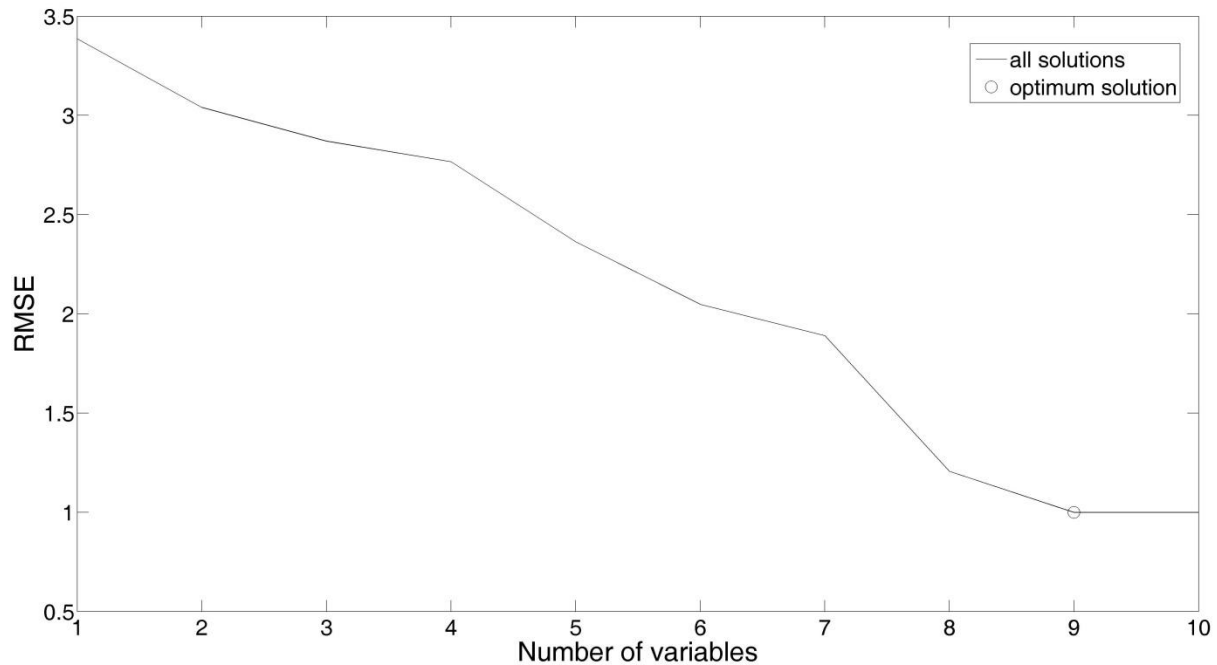


Figure 4.6 RMSE as a function of optimum combination of parameters used in the multi-linear regression calculation/prediction of TI

The equation obtained for the prediction/calculation of TI, from the MLR calculations, visually illustrated in Figure 4.6, is:

$$\begin{aligned}
 \text{TI} = & -40751.39 + (0.15 \times \text{SP}) + (-9.33 \times \text{Proximate moisture content}) + (22.79 \times \text{Proximate ash} \\
 & \text{content}) + (-0.28 \times \text{Proximate volatile content}) + (407.64 \times \text{Ultimate C content}) + (399.08 \\
 & \times \text{Ultimate H content}) + (473.64 \times \text{Ultimate N content}) + (342.49 \times \text{Ultimate S content}) + \\
 & (406.10 \times \text{Ultimate O content})
 \end{aligned}$$

The comparison between the experimentally obtained TI values and TI values calculated with the above-mentioned equation is shown in Figure 4.7. From this comparison, it is evident that MLR can be successfully used to predict TI, using the proximate and ultimate analysis values, as well as SP value.

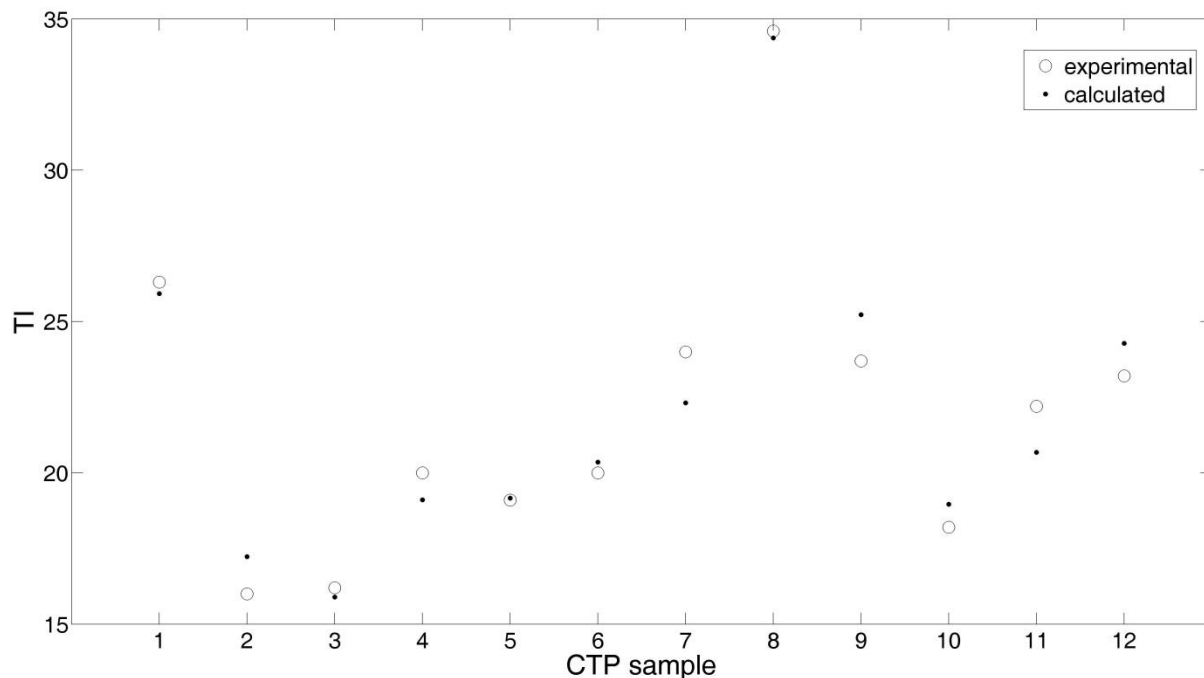


Figure 4.7 Comparison of TI values determined experimentally and those calculated utilising multi-linear regression

4.3.3 Multi-linear regression to calculate/predict QI

Figure 4.8 illustrates the optimum number of variables determined to minimise the RMSE during the MLR calculation for QI. From this figure, the optimum number of variables was determined as 7. These variables were SP, Moisture Content, Volatiles, C, H, N and O.

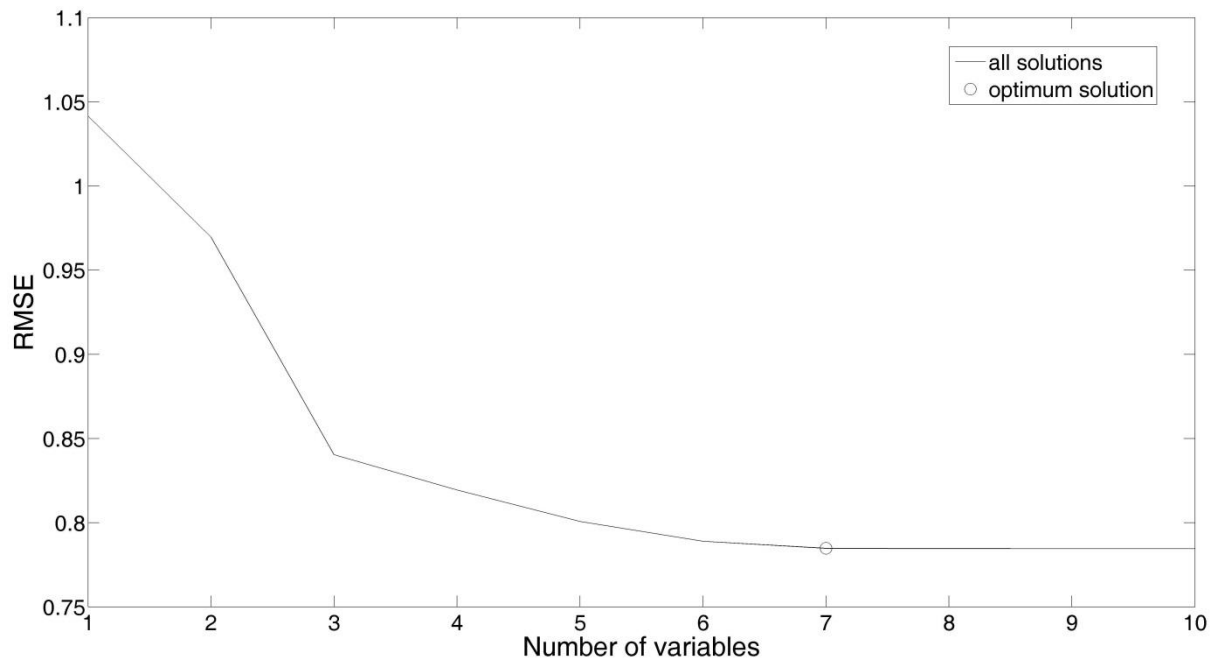


Figure 4.8 RMSE as a function of optimum combination of parameters used in the multi-linear regression calculation/ prediction of QI

The MLR equation obtained for the optimum solution to predict the QI values was:

$$\text{QI} = -1323.20 + (-0.02 \times \text{SP}) + (-1.56 \times \text{Proximate moisture content}) + (-0.10 \times \text{Proximate volatile content}) + (13.51 \times \text{Ultimate C content}) + (10.51 \times \text{Ultimate H content}) + (14.55 \times \text{Ultimate N content}) + (14.76 \times \text{Ultimate O content})$$

Using the above equation, QI could be calculated and compared against the experimental values. The comparison between the two sets of values is represented in Figure 4.9. From this comparison, it is obvious that MLR could be used to predict/calculate QI values. The calculated values correlated very well for some samples (e.g. CTP 3, 8 and 12), but were significantly different for CTP 7, 9, 10 and 11.

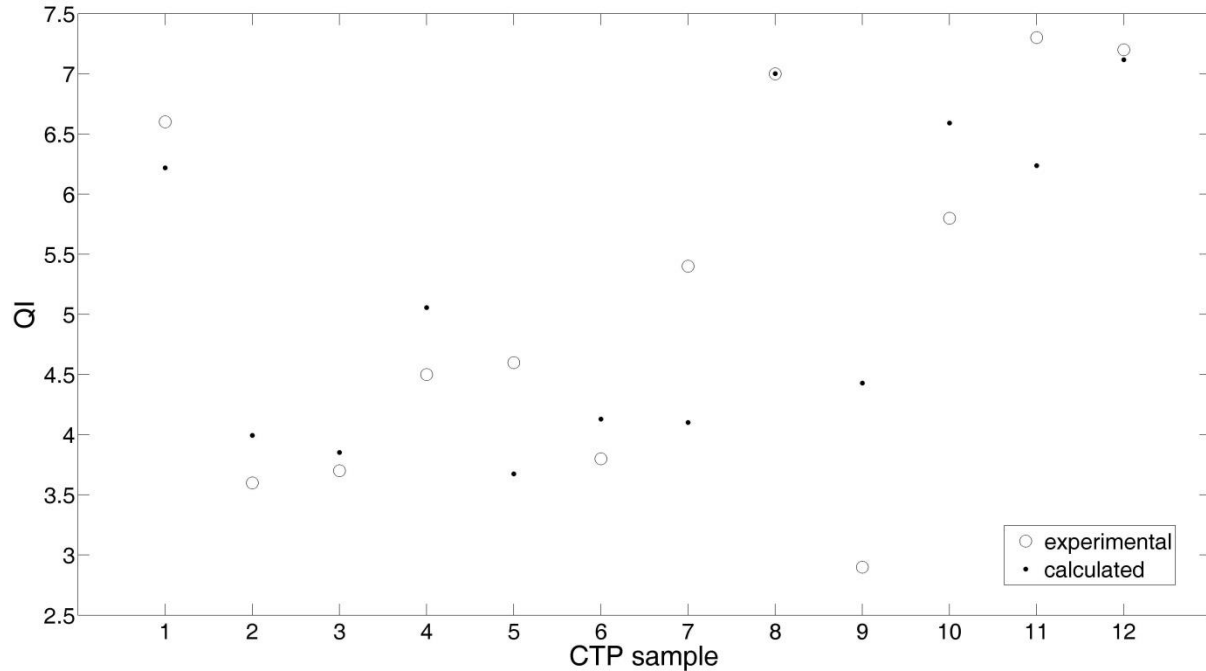


Figure 4.9 Comparison of QI values determined experimentally and those calculated utilising multi-linear regression

4.4 Conclusions

A comprehensive characterisation of 12 CTP samples was presented in this chapter. Although useful information can be obtained by such detailed characterisation, it is not common practice to characterise CTPs in such detail in industry. Therefore, the hypothesis was tested whether MLR could be used to predict or calculate less commonly determined characteristics from the more commonly obtained parameters. To test this theory, MLR using only the proximate and ultimate analyses, as well as SP values, were used to predict and calculate CV, TI and QI values. It was found that MLR could be used successfully to calculate CV (Section 4.3.1) and TI (Section 4.3.2), but less so for QI (Section 4.3.3). In order to understand the ability of MLR to predict/calculate the afore-mentioned parameters, it is important to understand the nature of these parameters in depth.

The CV value for a CTP is determined by means of the pyrolysis of a CTP in an inert atmosphere (Section 3.2.2). This experimental setup leads to results that can systematically be related to the ability of the specific CTP to form coke bridges and/or rigid carbon forms. The systematic nature of the CV values makes it more likely that it can be predicted and calculated with MLR. In contrast, the QI content of a CTP is also determined by non-systematic factors. Coke oven-derived QI can be divided into two types: normal (or primary) QI, and carry-over QI [Baron et al., 2009]. Normal QI is formed by thermal cracking of the coal tar pitch volatiles in the coke oven [Baron et al., 2009]. Normal QI has a very small particle size of approximately 1 micron and has a very high carbon-to-hydrogen ratio [Baron et al., 2009]. Carry-over QI is a result of the entrainment of solid particles in the coal volatiles as they are formed. Carry-over QI includes ash, coal particles, and coke cenospheres [Baron et al., 2009]. The carry-over fraction of QI will be different for each coke oven and it might change with altering operational conditions. The carry-over QI fraction should therefore be regarded as a non-systematic characteristic. This makes MLR prediction/calculation of QI less accurate, since MLR is a method of exploring the systematic nature of results. Since the TI content of a CTP also contains the QI content, the TI content can be regarded as being influenced by both systematic and non-systematic characteristics. Its prediction or calculation with MLR is therefore more accurate than for the QI, but not as accurate as for systematic parameters such as CV.